BIOCHEMISTRY
including biophysical chemistry & molecular biology

Article

pubs.acs.org/biochemistry

Facile Heme Vinyl Posttranslational Modification in a Hemoglobin

Matthew R. Preimesberger, Belinda B. Wenke, Lukas Gilevicius, Matthew P. Pond, and Juliette T. J. Lecomte*

T. C. Jenkins Department of Biophysics, Johns Hopkins University, Baltimore, Maryland 21218, United States

Supporting Information

ABSTRACT: Iron-protoporphyrin IX, or *b* heme, is utilized as such by a large number of proteins and enzymes. In some cases, notably the *c*-type cytochromes, this group undergoes a posttranslational covalent attachment to the polypeptide chain, which adjusts the physicochemical properties of the holoprotein. The hemoglobin from the cyanobacterium *Synechocystis* sp. PCC 6803 (GlbN), contrary to the archetypical hemoglobin, modifies its *b* heme covalently. The posttranslational modification links His117, a residue that does not coordinate the iron, to the porphyrin 2-vinyl substituent and forms a hybrid *b*/*c* heme. The reaction is an electrophilic addition that occurs spontaneously in the ferrous state of the protein. This apparently facile type of heme modification has been observed in only two cyanobacterial GlbNs. To explore the determinants of the reaction, we examined the behavior of *Synechocystis* GlbN variants containing a histidine at position 79, which is buried against the porphyrin 4-vinyl substituent. We found that L79H/H117A GlbN bound the heme weakly but nevertheless formed a cross-link between His79 Nε2 and the heme 4-Cα. In addition to this linkage, the single variant L79H GlbN also formed the native His117−2-Cα bond yielding an unprecedented bis-alkylated protein adduct. The ability to engineer the doubly modified protein indicates that the histidine−heme modification in GlbN is robust and could be engineered in different local environments. The rarity of the histidine linkage in natural proteins, despite the ease of reaction, is proposed to stem from multiple sources of negative selection.

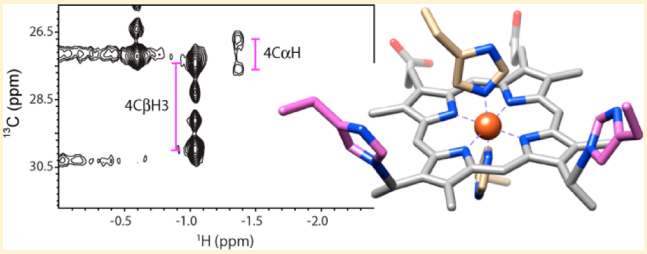

Hemoproteins are remarkable for both the chemistry that they perform and the chemistry that they avoid. The exquisite control exerted by the polypeptide chain on the high intrinsic reactivity of ferrous iron-protoporphyrin IX [*b* heme (Figure 1A)] is well-known and is often illustrated by contrasting proteins that favor reversible ligand binding (e.g., hemoglobin), O_2 activation and O transfer (e.g., cytochrome P450), or electron transport (e.g., cytochrome b_5).[1] The nature of the axial ligands to the iron, most commonly, histidine, methionine, and cysteine, is a primary determinant of essential heme properties such as reduction potential and capacity for electron transfer. Reactivity also extends to and is modulated by covalent attachment of the heme to the protein matrix, a characteristic of *c*-type cytochromes[2,3] and many mammalian peroxidases.[4,5]

Multiple functional roles are adopted by members of the hemoglobin superfamily;[6] as a result, these proteins are well suited for a focused inspection of heme chemistry diversification over evolutionary time. Known hemoglobins all utilize an unmodified *b* heme. Exceptions to this rule are found in the Group I 2/2 hemoglobins from the cyanobacteria *Synechocystis* sp. PCC 6803 and *Synechococcus* sp. PCC 7002. Specifically, these two proteins (GlbNs) undergo a spontaneous posttranslational modification (PTM) by which a noncoordinating histidine near the C-terminus (His117) reacts irreversibly with the heme 2-vinyl substituent to form a His117 Nε2−Cα linkage (Figure 1B).[7] In *Synechococcus*, there is evidence that the linkage is generated in vivo under microoxic growth conditions,[8] and the expectation is that the posttranslationally modified protein is functional in *Synechococcus* and *Synechocystis*. According to the current view, both GlbNs have a physiological role in reactive nitrogen species stress response.[8,9]

The most common heme−protein covalent linkage is the thioether bond found in *c*-type cytochromes,[2,3] where cysteines (generally two, occasionally one) play a role similar to that of the reactive histidine of GlbN (Figure 1E). In multiheme *c*-type cytochromes, covalent heme attachment is thought to allow for dense packing of the prosthetic groups and their controlled orientation.[10] In GlbN and monoheme *c*-type cytochromes, however, the necessity and consequences of the heme−protein linkage are not well understood.[8,11−14] Among proposed possibilities for GlbN are stabilization of the holoprotein[15,16] and heme sequestration.[17] The attachment of the cofactor may also weaken the constraints on protein stability during evolutionary selection and allow for a broad tuning of functional properties such as electron transfer and reduction potential.[12,18] Modification of redox properties is apparent in other heme PTMs[5] and can contribute in GlbN as well.[16,19] A characterization of the chemistry underlying the formation of

Received: March 6, 2013
Revised: April 19, 2013
Published: April 22, 2013

   dx.doi.org/10.1021/bi400289e | *Biochemistry* 2013, 52, 3478−3488

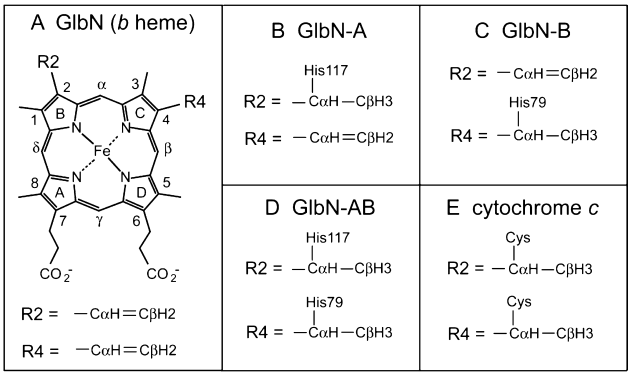

Figure 1. Chemical structure of *b* heme and covalently modified hemes discussed in the text. (A) The *b* heme has vinyl groups at positions 2 and 4. Protoporphyrin IX has a pseudo-C_{2v} axis of symmetry passing through the $\alpha-\gamma$ meso positions. Heme orientational isomerism arises from a 180° rotation about this axis. (B) The heme in GlbN-A has a bond between His117 Nε2 and 2-Cα. (C) The heme in GlbN-B has a bond between His79 Nε2 and heme 4-Cα. (D) The novel heme in GlbN-AB has the linkages found in both GlbN-A and GlbN-B. (E) The *c* heme in *c*-type cytochromes has thioether linkages at the 2-Cα and 4-Cα positions through conserved cysteines.

the GlbN linkage and its roles will therefore have implications for describing the evolution of heme proteins.

In previous work, we have exposed several features of the in vitro PTM mechanism (Scheme S1 of the Supporting Information).[19,20] The reaction occurs in the ferrous state and is initiated by protonation of the heme 2-vinyl Cβ atom by His117. Rapid nucleophilic attack of the heme 2-vinyl Cα atom by the now neutral histidine follows, generating an adduct with *R* stereochemistry at Cα. In the past, we explored the reactivity determinants that may be specific to GlbN. For example, in the absence of exogenous ligands, GlbN His46 (distal) and His70 (proximal) are axial ligands to the heme iron, but replacement of the distal histidine (His46) with a noncoordinating residue does not prevent the modification.[21] In addition, reaction in wild-type GlbN and its distal variants occurs when cyanide is bound to the ferric state prior to reduction. His46 replacement and cyanide binding are perturbations that permit formation of a product in which the minor heme orientational isomer [related to the major isomer by a 180° flip about the $\alpha-\gamma$ meso axis (Figure 1A)] reacts to generate a His117 adduct to the vinyl group on pyrrole C (4-vinyl).[20,21] Thus, the modification displays a degree of insensitivity to heme binding geometries and distal ligation.

The mechanistic features described above suggest that it should be possible to engineer the histidine–vinyl modification in different protein contexts. Achieving this goal would not only generate a deeper understanding of the PTM but also offer guidance in the design of stable proteins containing a nondisplaceable heme. We begin an exploration of the modification by focusing on *Synechocystis* GlbN and probing 4-vinyl reactivity with an engineered histidine. As we will show, the successful introduction of the histidine–heme linkage provides insight into heme chemistry and prompts a discussion of the rarity of the linkage in natural heme proteins.

MATERIALS AND METHODS

Materials. Horse skeletal myoglobin (Mb, >95% pure), horse heart cytochrome *c* (97%), sodium hydrosulfite (sodium dithionite, DT, ~85%), monobasic potassium phosphate, D_2O (99.9% ^2H), and $^{15}NH_4Cl$ (98% ^{15}N) were purchased from Sigma. Bovine hemin chloride (98%) and 2-butanone were obtained from Alfa-Aesar. Pyridine, dibasic sodium phosphate, and Tris base were obtained from Fischer; urea and ethylenediaminetetraacetic acid (EDTA) were obtained from EM Science, and $^{14}NH_4Cl$ was obtained from VWR. The chromatographic materials used to purify GlbNs were G-50 (fine) size-exclusion resin from Amersham BioScience, DEAE anion exchange resin from GE BioScience, and G-25 Sephadex desalting material from Sigma. Amicon Ultra (Millipore, molecular mass cutoff of 10 kDa) centrifugal filter units were used for protein concentration and buffer exchange.

Protein Production and Purification. A pET3c plasmid encoding H117A or wild-type *Synechocystis* GlbN was mutated by the QuikChange site-directed mutagenesis polymerase chain reaction (PCR) method (Qiagen, Valencia, CA) using primers purchased from IDT (Coralville, IA). Following DpnI digestion of the parent vector, the PCR product was used to transform DH5α *Escherichia coli* cells for plasmid preparation. Mutant pET3c plasmids encoding the single L79H or double L79H/H117A replacements in GlbN were purified using the Qiaprep spin miniprep kit (Qiagen) and positively confirmed by sequencing of the mutant genes (GENEWIZ, Inc., South Plainfield, NJ). These plasmids were used to transform BL21(DE3) *E. coli* for protein production.

Cells were grown in M9 minimal medium containing either $^{14}NH_4Cl$ or $^{15}NH_4Cl$ as the sole nitrogen source. Variant GlbN overexpression and purification were achieved as previously described for wild-type GlbN[20,22] with minor modifications. Because both L79H GlbN variants exhibit significantly attenuated heme affinity (vide infra), the heme addition step was completed last to prevent heme loss during DEAE anion exchange purification. Additionally, a higher-strength salt gradient (0 to 1 M NaCl) was used to elute variant apoproteins from the anion exchange column. Finally, purified (>95% by sodium dodecyl sulfate–polyacrylamide gel electrophoresis) variant GlbNs were exchanged from chromatography buffer [50 mM Tris and 5 mM EDTA (pH 8.2)] into storage buffer [~1 mM phosphate (pH ~7.5)]. Proteins prepared in this manner were either immediately examined for histidine–heme reactivity or lyophilized for long-term storage.

The UV–visible spectra of freshly reconstituted ferric L79H/H117A and L79H GlbNs are presented in Figure S1 of the Supporting Information. The Soret maxima are located at 413 nm (L79H/H117A GlbN) and 414 nm (L79H GlbN). Both proteins exhibit Q-bands at ~539 nm (~563 nm shoulder). These features are similar to those of wild-type GlbN (Soret band at 410 nm, Q-bands at ~546 nm) and are consistent with low-spin bis-histidine complexes at pH 7.1 and room temperature. Both L79H GlbN variants reconstituted using this method displayed $Abs_{(Soret)}/Abs_{(280\ nm)}$ ratios of approximately 4–5 (Figure S1 of the Supporting Information), similar to those of wild-type GlbN preparations. Concentrations were estimated optically with wild-type coefficients: ε_{278} = 7.4 mM^{-1} cm^{-1} for the apoprotein,[22] and ε_{410} = 100 mM^{-1} cm^{-1} for unreacted ferric GlbNs.[23]

L79H/H117A and L79H GlbN Reduction Reactions. The addition of histidine to a vinyl group causes a small blue shift in the reduced spectrum that can be monitored optically. Concentrated stock GlbN solutions were diluted into 100 mM phosphate buffer (pH 7.2) to yield ~10 μM GlbN, and reduction reactions were initiated by addition of freshly prepared DT (final concentration of ~2 mM). Manual mixing

dx.doi.org/10.1021/bi400289e | *Biochemistry* 2013, 52, 3478–3488

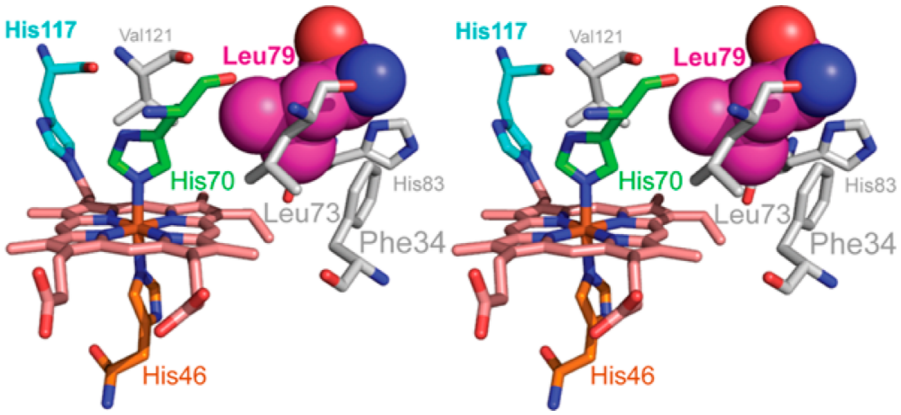

Figure 2. Stereoview (wall-eyed) of the proximal GlbN-A heme pocket (PDB entry 1RTX). Leu79 is shown as purple spheres. Its position with respect to the heme 4-vinyl group is similar to that of His117 (cyan sticks) with respect to the reacted 2-vinyl group. The side chains of Leu73, Phe34, His83, and Val121 (gray sticks) pack near Leu79. The axial iron ligands are shown as green sticks (proximal, His70) and orange sticks (distal, His46).

dead times were 15−20 s. For nuclear magnetic resonance (NMR) investigation, concentrated (~1 mM) GlbN samples were treated with a 5-fold molar excess of DT for 2−3 h, followed by $K_3[Fe(CN)_6]$ oxidation to the ferric state, and G-25 desalting into the desired buffer. In some cases, centrifugal filter units were used to reconcentrate and further exchange the sample into D_2O. Final protein NMR sample concentrations ranged from 1 to 5 mM. Apomyoglobin (apoMb) was prepared by extraction of heme from the acidified horse skeletal Mb (Sigma) with cold butanone,[24] followed by extensive dialysis of the soluble apoprotein against 1 mM phosphate. The amount of remaining Mb was estimated to be <5% based on UV−visible absorbance.

Pyridine Hemochromogen Assay. As a rapid test for heme modifications, the hemochromogen assay[25] was performed as previously reported.[20] DT-reacted samples were typically reduced for 1−2 h to allow for complete conversion prior to the samples being assayed. The results were interpreted by comparison with published spectra (α and β band maxima).[26,27]

Optical Spectroscopy. Absorbance spectra were recorded on a Varian Cary50 instrument for monitoring the kinetics of heme modification reactions. Spectra were collected from 640 to 350 nm, in 1 nm steps, using a 0.1 s averaging time. The hemochromogen assay results were read on an Aviv 14-DS spectrophotometer, equipped with a Peltier device set to 25 °C, from 600 to 500 nm, in 0.5 nm steps (0.5 nm slit width), using an averaging time of 1 s. The presented pyridine hemochrome spectra are the average of three consecutive scans. The same Aviv 14-DS instrument was used for thermal heme loss experiments. Temperature-dependent spectra were colledcted in triplicate from 700 to 280 nm, in 1 nm steps (1 nm slit width), using a 0.2 s averaging time. Spectra were recorded with ~10 μM GlbN samples, in 250 mM degassed phosphate buffer (pH 7.3), from 25 to 91 °C, in 3 °C steps, each following a 5 min thermal equilibration period. Because all samples exhibit irreversible transitions, variable-temperature data were interpreted qualitatively.

NMR Spectroscopy. All data were collected at 600 MHz on Bruker AVANCE or AVANCE-II spectrometers equipped with cryoprobes. The probe temperature was calibrated using methanol.[28] NMR experiments used to establish the heme pocket environment and covalent structure of the variant heme modifications were as previously reported[15,20] and included ^{1}H one-dimensional, ^{1}H−^{1}H DQF-COSY, ^{1}H−^{1}H TOWNY TOCSY,[29] water presaturation ^{1}H−^{1}H NOESY, water elimination Fourier transform (WEFT) ^{1}H−^{1}H NOESY,[30] ^{1}H−^{15}N HSQC, ^{1}H−^{15}N long-range (lr) HMQC,[31] natural abundance ^{1}H−^{13}C HMQC, and natural abundance band-selective ^{1}H−^{13}C HSQC with or without ^{1}H decoupling. Data were processed using either TopSpin 2.1 (Bruker BioSpin, Rheinstetten, Germany) or NMRPipe.[32] Processed spectra were analyzed using Sparky 3.[33] ^{1}H chemical shifts were referenced to DSS through the temperature-corrected water line (4.76 ppm at 298 K); ^{13}C and ^{15}N chemical shifts were referenced indirectly using Ξ ratios.[34]

Database Analysis. A list of Protein Data Bank (PDB) files[35] was obtained from the RCSB site[36] using HEM as a ligand keyword. The 95% similarity filter option was applied, and proteins containing a thioether bridge to a HEM ligand were discarded. If an artificial variant was selected in the set, it was removed and replaced with the corresponding wild-type structure. If a wild-type structure was not available, the protein was eliminated from the set. The resultant data set was composed of 341 structures, with PDB entries listed in Table S3 of the Supporting Information. The set contained 28% globins, 23% cytochromes P450, and a variety of other cytochromes, catalases, peroxidases, etc. The BioPython module[37] was used to identify noncoordinating residues with a Cα atom within 7 Å and a Cβ atom within 6 Å of a HEM vinyl Cα or propionate Cα atom and to count the total number of residues. The propensity P_i^v of amino acid of type i to satisfy the vinyl (v) distance criteria was estimated using

$$P_i^v = \frac{N_i^v / \sum_j N_j^v}{N_i / \sum_j N_j}$$

where N_i^v represents the number of amino acids of type i identified near a vinyl in the set and N_i represents the total number of amino acids of type i in the heme domains of the set. The index j covers all amino acids.

RESULTS

The crystal structure of *Synechocystis* GlbN with a heme covalently attached (GlbN-A, PDB entry 1RTX,[38] Figure S2 of the Supporting Information) was used to identify a position

appropriate for the placement of a histidine for reaction with the heme 4-vinyl. Of the few residues located in the proximity of the 4-vinyl substituent, semiconserved Leu79 was selected because its orientation is analogous to that of His117 with respect to the 2-vinyl (Figure 2). Furthermore, position 79 resides in the FG corner, which may tolerate some extent of backbone relaxation.

Properties of L79H/H117A GlbN. The apoprotein of GlbN partitions primarily into inclusion bodies. The holoGlbN preparation therefore includes a heme titration step, typically performed before purification by anion exchange chromatography.[22] When this protocol was applied to the variant, most of the heme dissociated from the apoprotein during its passage through the column. According to optical data, increasing or decreasing the pH from neutrality led to increases in high-spin heme characteristics (shoulder at ~375 nm, charge transfer band at ~620 nm, data not shown). Because the H117A replacement has no such consequences on its own,[39] we concluded that the ferric heme affinity was significantly compromised by the L79H replacement. To circumvent this issue, heme was added in a stoichiometric amount to the apoprotein after the chromatographic steps.

The resistance of L79H/H117A GlbN to thermally induced heme loss was monitored by absorbance spectroscopy (Figure S3 of the Supporting Information). As the temperature is increased above 25 °C, a charge-transfer band emerges at ~610 nm, providing evidence of deligation of His46 and the population of a high-spin complex. The magnitude of the Soret band decreases gradually, and eventually, the spectrum changes into that of free ferric heme. Under the conditions assayed (~10 μM protein, pH 7.3, and 250 mM phosphate buffer), the thermal transition is irreversible, and thermodynamic parameters characterizing the process were not obtained. Heme loss occurs with low cooperativity and an apparent midpoint of ~52 °C, ~20 °C lower than that of wild-type GlbN.[22]

^{1}H NMR spectroscopy was used to characterize ferric L79H/H117A GlbN prior to treatment with the reducing agent. The spectrum, shown in Figure 3C, can be compared to that of wild-type GlbN without histidine−heme PTM (Figure 3A). Although the chemical shifts of resolved resonances are similar, L79H/H117A GlbN exhibits much broader lines than the wild-type protein across the whole spectrum. The excess line width is attributed to exchange among various paramagnetic species: partially folded apoprotein with nonspecifically bound heme and bis-histidine holoprotein. NMR data reveal the largest population of low-spin species at neutral pH in agreement with the optical data. The study of ferric L79H/H117A GlbN was not pursued because of its inferior NMR spectral properties.

Heme Modification in L79H/H117A GlbN Monitored Optically. The response of L79H/H117A GlbN to reduction with DT was monitored as a function of time by absorption spectroscopy in the visible range (Figure 4), as was done for the wild-type protein.[20] In a first set of experiments, ~10 μM L79H/H117A GlbN was treated with a 200-fold molar excess of DT in 100 mM phosphate (pH 7.1), and spectra were collected from 350 to 640 nm for several hours. Reduction, which is essentially complete during the manual mixing dead time (~15 s), is manifested in the Soret maximum of approximately 426 nm, with an α band at 560 and a β band at 531 nm (Figure 4A, red trace). Interestingly, further spectral changes are observed, and after 1 h, the sample exhibits Soret, α, and β bands at 424, 558, and 528 nm, respectively, all blue-

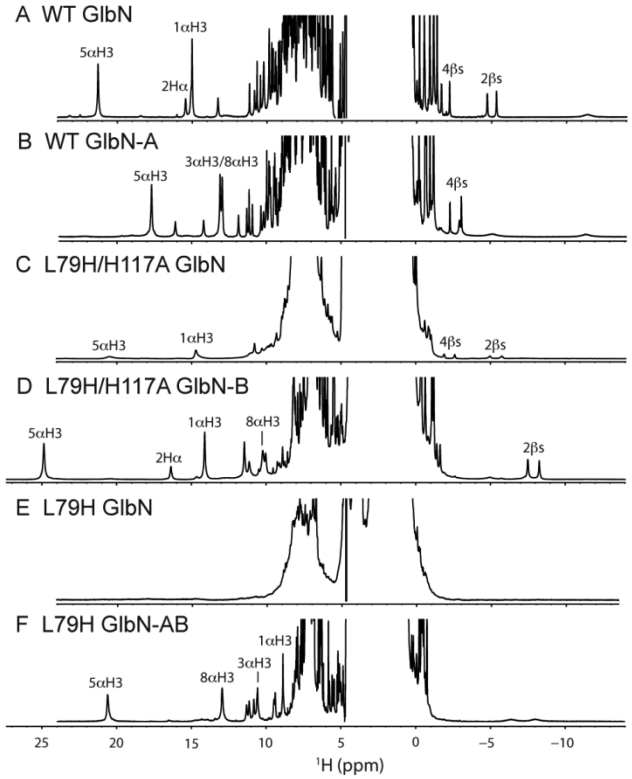

Figure 3. ^{1}H NMR spectra of various ferric GlbNs. (A) Wild-type GlbN and (B) wild-type GlbN-A are included for reference (pH 7.2, 298 K). (C) L79H/H117A GlbN (pH 7.3, 298 K). (D) L79H/H117A GlbN-B (pH* 7.0, 298 K, 99.9% D_2O). (E) L79H GlbN (pH 7.3, 298 K). (F) L79H GlbN-AB (pH* 7.6, 313 K, 99.9% D_2O). The complexes are paramagnetic ($S = {}^1/_2$) with bis-histidine iron coordination; in panels C and E, a contribution of high-spin ($S = {}^5/_2$) and apoprotein species is likely. Selected heme assignments are as indicated (see Tables S1 and S2 of the Supporting Information for chemical shift values).

shifted compared to those of the initial ferrous state (Figure 4A, cyan trace). Also of note is the initial decrease in Soret intensity, because reduced bis-histidine GlbNs generally have α, β, and Soret extinction coefficients larger than those in the corresponding oxidized state.

A second set of experiments was performed to identify the nature of the kinetic phases and the species involved. The L79H/H117A variant was again treated with a 200-fold molar excess of DT and mixed manually for ~15 s, but in this case, the reduction step was immediately followed by addition of a 2-fold molar excess of horse skeletal apomyoglobin (apoMb) as a heme scavenger. Within seconds of the addition of apoMb, an absorption band characteristic of deoxyMb[27] appeared in the spectrum (Figure 4B), and no obvious spectral component corresponding to ferrous GlbN remained. This demonstrated that the fast reduction phase results in a protein containing a noncovalently attached heme, and that dissociation of heme from this reduced state occurs rapidly.

In contrast, when L79H/H117A GlbN was incubated with reducing agent for 1 h to produce the species with a blue-shifted optical spectrum (Figure 4A, cyan trace), oxidized, and then retreated with excess DT, reduction led rapidly and directly to the blue-shifted spectrum. Addition of apoMb at this stage did not perturb the spectrum and confirmed that the heme is no longer transferrable (Figure 4C). These

dx.doi.org/10.1021/bi400289e | Biochemistry 2013, 52, 3478−3488

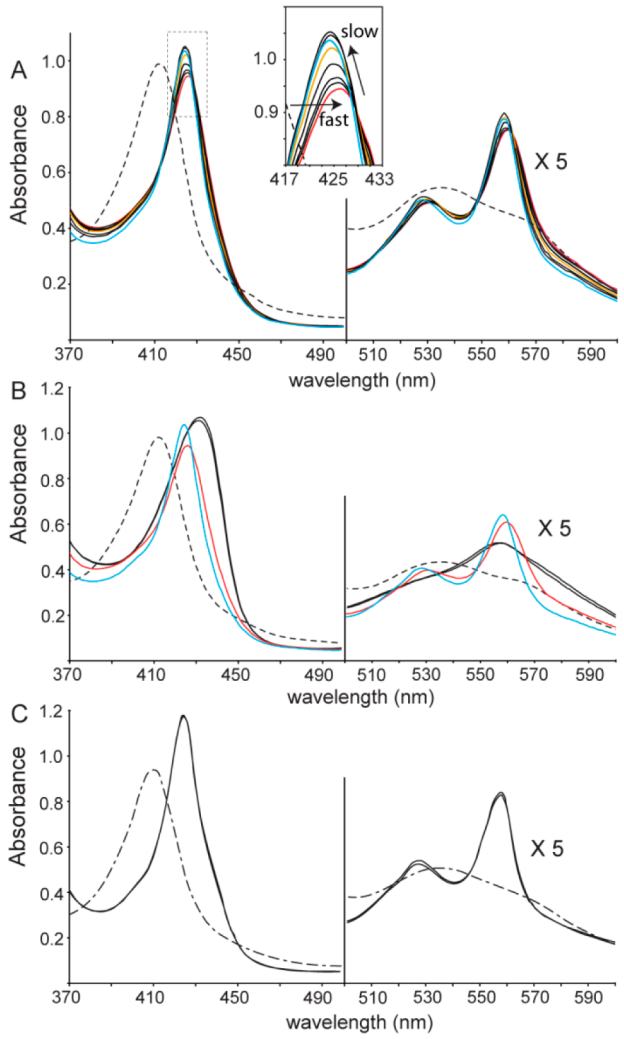

Figure 4. Time dependence of the absorbance spectrum of L79H/H117A GlbN after reduction with DT. Data were collected in the presence and absence of the heme scavenger horse skeletal apoMb. Conditions: ~10 μM GlbN, 100 mM phosphate, pH ~7.1, 2 mM DT, room temperature, dead time of 15–20 s. Spectra of (A) ferric GlbN (dashed), the intermediate ferrous form appearing during the dead time (red), and the product generated after 10 min (orange) and 1 h (cyan). The inset magnifies the Soret region. (B) Same experiment as in panel A, except that 20 μM apoMb was added immediately following reduction by DT. The initial spectrum (---) converted rapidly to that of deoxyMb [spectra shown after 15 s and 10 min (—)]. (C) Same as panel B, but with ferric GlbN-B as the starting material (–·–). No transfer of heme to apoMb was observed [15 s and 10 min spectra shown (—)].

observations are consistent with the fast kinetic phase corresponding to reduction of the *b* heme and the slow phase reflecting its irreversible attachment to the protein.

To inspect the integrity of the heme group, we first used the pyridine hemochromogen assay.[25] This method eliminates the influence of tertiary structure on optical properties by denaturing the protein in basic pyridine. Subsequent reduction yields a bis-pyridine ferrous heme complex with absorption maxima characteristic of various heme modifications. Figure S4A of the Supporting Information presents the pyridine hemochrome spectra of untreated and DT-reacted L79H/H117A GlbN. As expected, the untreated variant yields the spectrum of bis-pyridine ferrous protoporphyrin IX (α and β band maxima at 557 and 525 nm, respectively). The reacted variant displays blue-shifted bands (553 and 523 nm), within error of those observed for wild-type GlbN-A[40] and confirming the saturation of one vinyl group. Henceforth, the product of the DT treatment is denoted as L79H/H117A GlbN-B.

Characterization of Ferric GlbN-B by NMR Spectroscopy. Several adducts are a priori consistent with the results described above, involving the vinyl Cα atom as in GlbN-A or the Cβ atom as in the cytochrome *c* maturation protein CcmE,[41] and the histidine Nε2 (GlbN-A) or Nδ1 (CcmE) atom. Other heme modifications, caused by side reactions with DT byproducts, are also possible. Homo- and heteronuclear NMR data were collected to determine the nature of the heme–protein linkage.

The ^{1}H NMR spectrum of ferric L79H/H117A GlbN-B is shown in Figure 3D. Compared to those of the starting material (Figure 3C), the distinct chemical shifts confirm that a reaction has gone to completion. In addition, the resolved lines in the GlbN-B spectrum are sharp and their chemical shift is consistent with a well-folded, low-spin, bis-histidine complex such as GlbN-A (Figure 3B). The small number of paramagnetically shifted lines also suggests that a single product has been obtained.

In addition to the engineered His79 in the FG turn, L79H/H117A GlbN contains five histidines: the proximal (His70) and distal (His46) axial ligands, His33, His77, and His83 (Figure S2 of the Supporting Information). To examine these side chains, we used a uniformly ^{15}N-labeled sample of ferric L79H/H117A GlbN-B and collected ^{15}N band-selective ^{1}H–^{15}N long-range (lr) HMQC spectra (Figure 5A). The assignments of Hδ2, Hε1, ^{15}Nδ1, and ^{15}Nε2 in His83, His33, and His77 are readily transferred from wild-type GlbN-A.[7] The ^{1}H–^{15}N lr HMQC spectrum exhibits an unusual pair of cross-peaks indicating that an aromatic nitrogen (^{15}N at 205.5 ppm) is covalently connected to two sets of protons resonating upfield, at 2.88 and −1.04 ppm (Figure 5A). Because signals from the iron axial ligands (His46 and His70) are efficiently relaxed by paramagnetism and not detected in this experiment,[7] the unusual spin system is attributed to a moiety that is either part of a modified His79 or connected to it.

^{1}H–^{1}H NOESY, ^{1}H–^{1}H DQF-COSY, ^{1}H–^{1}H TOCSY, and natural abundance ^{1}H–^{13}C HMQC spectra were collected to assign the heme ^{1}H and ^{13}C resonances. Four heme CαH$_3$ signals (Figure S5 of the Supporting Information) are identified by their intensity, downfield-shifted ^{1}H resonances, and upfield-shifted ^{13}C resonances.[15] DQF-COSY signals at 16.42, −7.45, and −8.21 ppm correspond to the α, β(*trans*), and β(*cis*) protons of one vinyl group, respectively (Figure S6A of the Supporting Information). The β protons exhibit strong NOEs to a heme CαH$_3$ [δ(^{1}H) = 14.17 ppm], itself in contact with another heme CαH$_3$ [δ(^{1}H) = 10.28 ppm (Figure S6B–D of the Supporting Information)]. The latter heme methyl shows NOEs to a set of four *J*-coupled protons belonging to a heme propionate. These connectivities assign the heme 1-CαH$_3$, 8-CαH$_3$, and 7-propionate (Figure 1A) and demonstrate that GlbN-B contains an intact 2-vinyl group. NOEs between the 2-vinyl CβH(*trans*) and the 1-CαH$_3$ (Figure S6C of the Supporting Information), and between the 2-vinyl Hα and the heme α-meso proton (not shown), define the orientation of the vinyl group in the heme plane as "*trans*".[42]

The heme 3-CαH$_3$ [δ(^{1}H) = 6.87 ppm] exhibits a strong NOE to the signal observed at δ(^{1}H) = −1.04 ppm in the ^{1}H–^{15}N lr HMQC spectrum (Figure 5A and Figure S6I of the

dx.doi.org/10.1021/bi400289e | *Biochemistry* 2013, 52, 3478–3488

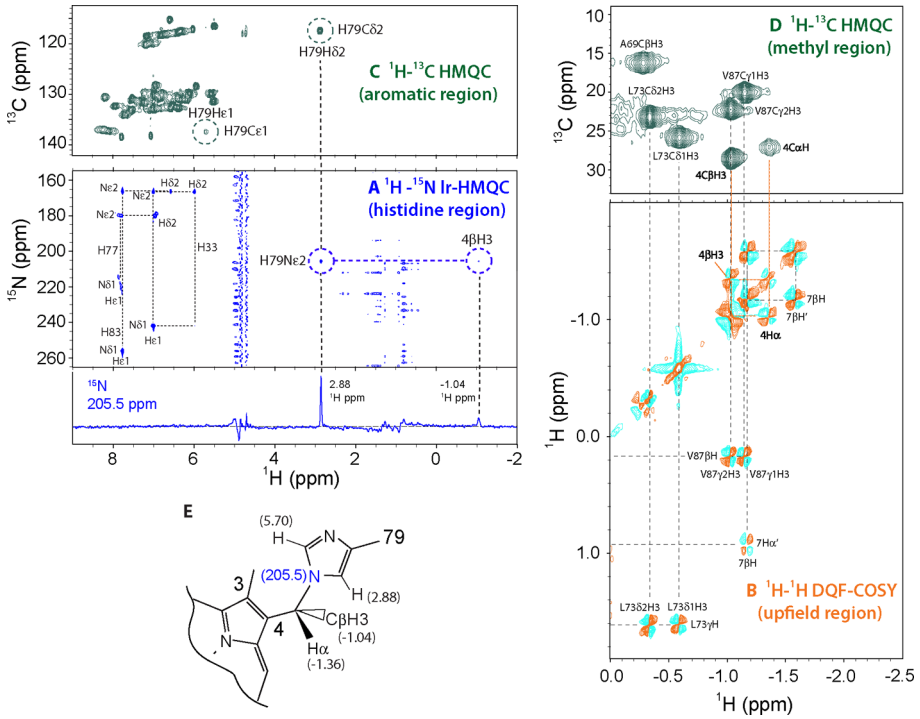

Figure 5. Identification of the heme modification in ferric L79H/H117A GlbN-B. (A) ^{1}H−^{15}N lr HMQC spectrum highlighting an unusual pair of proton signals (2.88 and −1.04 ppm) with a common ^{15}N shift at 205.5 ppm. (B) Portion of the ^{1}H−^{1}H DQF-COSY data showing a *J* connectivity between the protons at −1.04 and −1.36 ppm. Signals corresponding to Val87, Leu73, and 7-propionate spin systems are also labeled. (C) Aromatic region of the natural abundance ^{1}H−^{13}C HMQC spectrum identifying the signal at 2.88 ppm (^{1}H shift) as His79 Hδ2 atom through its directly attached Cδ2 atom (117.5 ppm). The His79 Cε1 correlation is also circled. (D) Methyl region of the natural abundance ^{1}H−^{13}C HMQC spectrum showing resolved ^{13}C shifts for the 4CβH$_3$−CαH pair. (E) Structure of posttranslational modification consistent with the data. ^{1}H−^{1}H and ^{1}H−^{13}C data were acquired for ∼5 mM ferric L79H/H117A GlbN-B at pH* 7.04 and 298 K in 99.9% D_2O; ^{1}H−^{15}N data were acquired for an ∼1 mM ^{15}N-labeled GlbN-B sample at pH 7.62 and 298 K in H_2O.

Supporting Information). This proton (or set of protons) is *J*-correlated to proton(s) resonating at −1.36 ppm (Figure 5B). ^{1}H−^{13}C cross-peaks corresponding to the pair at −1.36 and −1.04 ppm are resolved (Figure 5D), so that their multiplicity can be determined with a ^{13}C band-selective ^{1}H−^{13}C HSQC experiment conducted without ^{1}H decoupling in the indirect dimension (Figure S7 of the Supporting Information). The signal at −1.04 ppm is a quartet, whereas the signal at −1.36 ppm is a doublet, both with a $^1J_{CH}$ value of ∼130 Hz. Thus, the pattern indicates a CαH−CβH$_3$ system, and the proximity to the 3-CαH$_3$ confirms the modification of the 4-vinyl group. The remaining heme signals are assigned as usual with a combination of ^{1}H and ^{13}C data.

The last step in the structure determination is the characterization of the modified His79 and its bond to the heme. According to the ^{1}H−^{13}C HMQC spectrum, the proton at 2.88 ppm [lr correlation to a ^{15}N at 205.5 ppm (Figure 5A)] is directly bonded to a ^{13}C resonating at 117.5 ppm (Figure 5C). This shift is consistent with a histidine Cδ2,[43] and it assigns the ^{15}N signal as the Nε2 atom of His79. Furthermore, the ^{1}H−^{1}H TOCSY spectrum contains a connectivity between 2.88 and 5.70 ppm, assigning the latter proton to His79 Hε1 (data not shown); accordingly, the His79 CεH1 direct correlation is present in the aromatic region of ^{1}H−^{13}C HMQC data [Figure 5C; δ(^{13}C) = 137.6 ppm]. The PTM covalent structure is therefore as depicted in Figure 5E. Strong dipolar contacts are observed between His79 Hδ2 and the 4-CαH−CβH$_3$ moiety (Figure S6K of the Supporting Information), and His79 Hε1 is in contact with both the 3-CαH$_3$ (not shown) and 4-CβH$_3$ substituents (Figure S6I of the Supporting Information). These effects are consistent with a conformation in which His79 Hε1 faces the heme 3-CαH$_3$ and His79 Hδ2 faces the heme 4-CαH/5-CαH$_3$ side of heme pyrrole C. Heme and reacted histidine chemical shifts are listed in Table S1 of the Supporting Information.

The composite NMR data establish that His79 reacts with the 4-vinyl substituent to form a Markovnikov adduct with *R* stereochemistry. The addition is analogous to the wild-type PTM and consistent with a reduction-driven reaction in which 4-Cβ protonation is followed by nucleophilic attack linking His79 Nε2 to the heme 4-Cα atom.[20]

Heme Environment in Ferric GlbN-B. Several Tyr and Phe side chains line the GlbN-B heme pocket and are in contact with the prosthetic group (Figure S6E−I of the Supporting Information). In addition, contacts between upfield-shifted aliphatic groups and heme (Figure S6I−L of the Supporting Information) orient the modified heme group unambiguously in the cavity of L79H/H117A GlbN-B. These effects are consistent with the crystallographic model of wild-type GlbN-A (PDB entry 1RTX[38]); no major structural change occurs within the heme pocket upon covalent attachment via the nonnative His79 linkage (Figure S6M of the Supporting Information). This is an important feature of GlbN-B because, on the basis of geometry alone, a histidine at position 117 should be able to react with the 2-vinyl in this singly modified protein. The hybrid *b*/*c* heme, however, is expected to have electronic properties different from those of a *b* heme.[12] Formation of histidine−heme linkages at both vinyl groups

dx.doi.org/10.1021/bi400289e | *Biochemistry* 2013, 52, 3478−3488

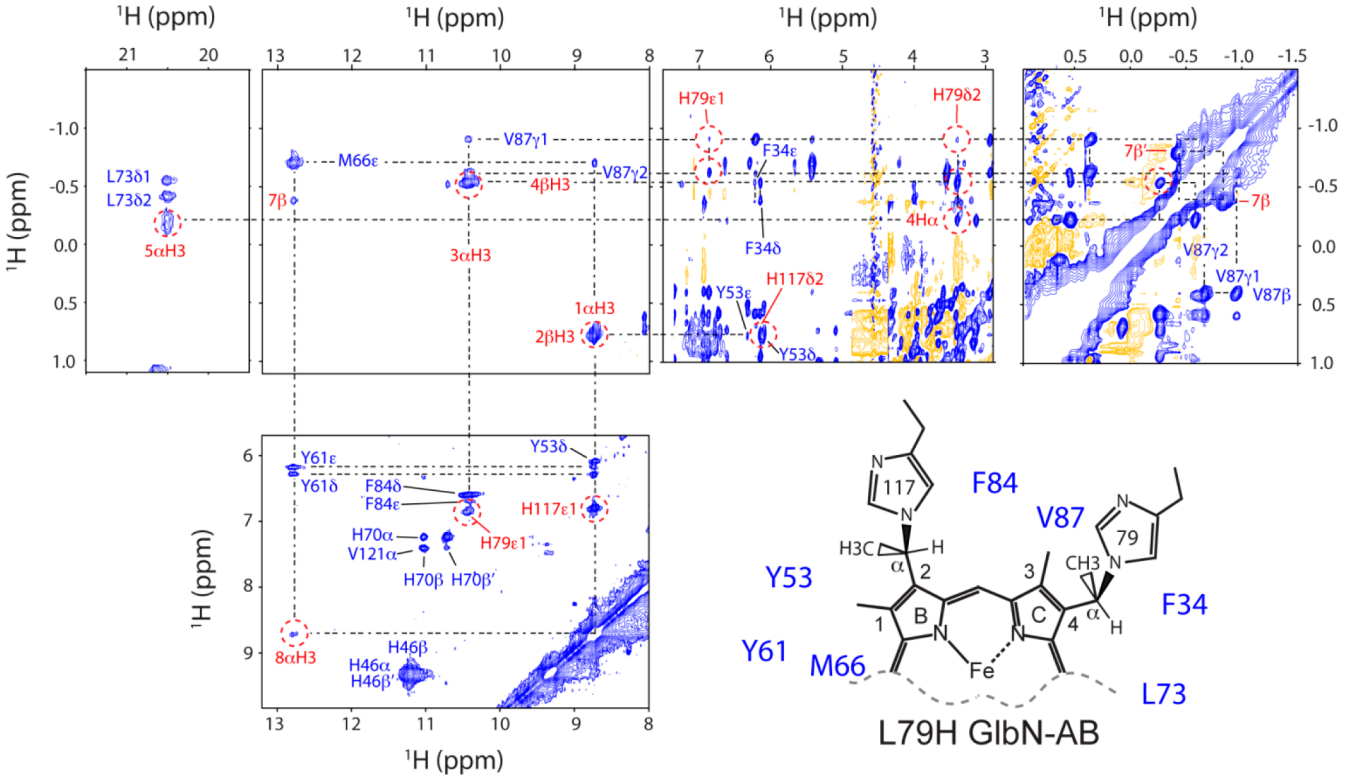

Figure 6. NOE contacts detected near the sites of modification within L79H GlbN-AB. As observed in L79H/H117A GlbN-B (Figure S6I,K of the Supporting Information), the heme 4-βH_3 signal (−0.57 ppm) exhibits strong cross-peaks with His79 Hδ2, Phe34 ring protons, and the heme 4-Hα and 3-αH_3 atoms. The 4-Hα resonance is in dipolar contact with His79 Hδ2, Phe34 Hδs (weak), and the heme 5-αH_3 group. On pyrrole B, the heme 2-βH_3 signal displays strong interactions with His117 Hδ2, the aromatic protons of Tyr53, and the heme 1-αH_3, itself in contact with Tyr53, Tyr61, Met66 εH_3, His117 Hε1, and the heme 8-αH_3. Signals derived from the modified heme are highlighted in red. The set of dipolar connectivities is consistent with *R* stereochemistry at both heme position 2 and 4 substituents (bottom right). Ferric L79H GlbN-AB NOESY data (τ_{mix} = 50 ms) were acquired on an ∼5 mM sample at pH* 7.61 and 313 K in 99.9% D_2O.

would provide additional clues about the mechanism and the robustness of the modification. We therefore attempted reaction with the single variant, L79H GlbN.

Properties of L79H GlbN. L79H GlbN loses ferric heme when it is passed through the anion exchange column and requires reconstitution with heme after apoprotein purification. The ^{1}H spectrum of ferric L79H GlbN, shown in Figure 3E, does not present obvious hyperfine-shifted lines and exhibits little chemical shift dispersion. The thermal response (data not shown) is within error of that of the double variant (Figure S3 of the Supporting Information).

Heme Modification in L79H GlbN Monitored Optically. Reduction of L79H GlbN as described for L79H/H117A GlbN yields qualitatively similar results. In the dead time of the experiment, a ferrous spectrum is obtained with maxima near 426, 560, and 531 nm (Figure S8 of the Supporting Information, red trace) and reduced intensity. A slow phase then leads to a second ferrous species with recovered Soret, α, and β bands at 420, 555 (∼550 sh), and 524 (∼530 sh) nm, respectively (Figure S8 of the Supporting Information, purple trace). These blue shifts were twice as large as those observed in the same experiment with L79H/H117A GlbN (Figure 4A) but occurred over a similar time scale (∼1 h).

The result of the hemochromogen assay performed on reacted L79H GlbN is shown in Figure S4B of the Supporting Information, along with that of cytochrome *c* for reference. The α and β bands of the bis-pyridine ferrous complex are detected at 550 and 520 nm, respectively. These values are similar to those of mesoheme and *c* heme (Figure S4B,C of the Supporting Information), chromophores in which both the position 2 and 4 substituents are saturated. Henceforth, the product of the L79H GlbN reaction will be termed GlbN-AB.

Characterization of Ferric GlbN-AB by NMR Spectroscopy. The NMR strategy described above for L79H/H117A GlbN-B was applied to ferric L79H GlbN-AB. The one-dimensional ^{1}H spectrum (Figure 3F) exhibits sharp lines and indicates the formation of a specific product. The ^{1}H−^{15}N lr HMQC spectrum (Figure S9 of the Supporting Information) contains signals arising from all five nonaxial histidines. Resonances corresponding to His83, His33, and His77 can be assigned by comparison to L79H/H117A GlbN-B data. Additionally, a pair of cross-peaks with a common ^{15}N shift (209.9 ppm) and ^{1}H shifts of 3.42 and −0.57 ppm provides initial evidence that His79 reacted as in GlbN-B. By elimination, His117 is responsible for the three remaining signals, at $\delta(^{15}N)$ = 248.1 ppm with two connectivities [$\delta(^1H)$ = 6.84 and 6.16 ppm] and $\delta(^{15}N)$ = 250.4 ppm with one connectivity [$\delta(^1H)$ = 6.84 ppm]. The ^{15}N shifts are comparable to those observed for His117 in wild-type GlbN-A[7] and are indicative of ^{15}N atoms without an attached proton.

The ^{1}H−^{13}C data identify the four heme CαH_3 resonances with characteristic upfield ^{13}C shifts (Figure S10 of the Supporting Information). The reacted position 4 substituent in GlbN-AB has ^{1}H and ^{13}C shifts similar to those in GlbN-B (Figure S11 of the Supporting Information). The 4-CβH_3 ^{1}H (−0.57 ppm) displays a strong NOE to the heme 3-CαH_3

dx.doi.org/10.1021/bi400289e | *Biochemistry* 2013, 52, 3478−3488

group [$\delta(^1H)$ = 10.44 ppm]. Other NOEs from the 4-CαH−CβH_3 unit to the heme and protein are similar to those observed in L79H/H117A GlbN-B and establish the orientation of the reacted His79 and *R* stereochemistry at 4-Cα (Figure 6).

Vinyl groups are conspicuous in $^1H-^1H$ DQF-COSY data of ferric bis-histidine GlbNs. The downfield-shifted CαH exhibits two strong upfield cross-peaks, one with a large $^3J_{HH}$ (~12−15 Hz) corresponding to the *trans* proton. No spin system consistent with an intact vinyl moiety was detected in the spectrum of ferric L79H GlbN-AB. Signals corresponding to His117 Cδ2 and Cε1 were identified in the $^1H-^{13}C$ HMQC spectrum (Figure S12 of the Supporting Information), along with a far downfield-shifted methyl group [$\delta(^{13}C)$ = 61.8 ppm (Figure S11 of the Supporting Information)], which was absent from GlbN-B spectra but present in wild-type GlbN-A and assigned to the 2-CβH_3. The attached protons (0.74 ppm) display strong NOEs to the heme 1-CαH_3 group [$\delta(^1H)$ = 8.75 ppm] and His117 Hδ2. In addition, NOEs involving the 1-CαH_3 and His117 Hε1 are as in wild-type GlbN-A and establish the presence of the linkage between His117 Nε2 and the heme 2-Cα (Figure 6). Heme and reacted histidine chemical shifts are listed in Table S2 of the Supporting Information.

We conclude that two histidine−heme covalent linkages can readily be created in GlbN. The reaction requires no enzyme, and a unique product is obtained with complete stereospecificity. To the best of our knowledge, alkylation of two histidines by a heme group has not been reported. This novel modification parallels the double thioether modification observed in the majority of *c*-type cytochromes.

Frequency of Histidine Occurrence near a Heme Vinyl Group. An analysis of 341 three-dimensional structures of proteins with at most 95% sequence similarity and containing a *b* heme (Table S3 of the Supporting Information) was performed to identify residues with a backbone Cα atom within 7 Å of a vinyl Cα atom and a side chain Cβ atom within 6 Å of the same vinyl Cα atom. These arbitrary thresholds were chosen to capture His117 and Leu79 in GlbN-A and be otherwise permissive considering that the distance between a histidine Cα atom and the tip of its imidazole ring is <5 Å in any rotameric state.

When the number of hits with vinyls (excluding iron-ligating residues) is normalized for the frequency of occurrence in the set, hydrophobic residues are found to be preferred in the following order: Val > Phe > Ile > Leu (Figure S13 of the Supporting Information). Thr is also preferred, along with Met and Tyr, two residues that can be oxidized and form heme adducts.[5,44] Perhaps unsurprising is the depletion of ionizable residues. The preference order is Asp ~ Lys < Glu < Cys < Arg < His (Asp and Lys being the rarest). Interestingly, each of the low-propensity side chains (except Arg) is documented to react covalently with the porphyrin macrocycle in various cytochromes and peroxidases.[4,5,44] Of direct relevance to this study are 40 histidines found near vinyl groups. A majority of the imidazole rings are involved in strong interactions (helix N-capping or salt bridge to a propionate), and none are poised for vinyl addition in the χ_1 rotameric state observed in the structures or alternative χ_1 rotameric states. When the same distance criteria are used with propionate instead of vinyl Cα atoms, His and Arg have high propensities, whereas Cys, Glu, and Asp are strongly avoided.

DISCUSSION

Structural and Chemical Criteria for Histidine−Vinyl Addition in GlbN. There are obvious geometric requirements for the histidine−heme modification to occur. The histidine Nε2 atom must be able to reach a vinyl Cα atom, and the local structure must be such that sp^3 bond angles can be established at that carbon. In our search for suitable positions in the X-ray structures of GlbN and proteins such as myoglobin and cytochrome b_5, we found the distance and angle criteria are difficult to satisfy simultaneously without global structural adjustments.

Position 79 in the X-ray structure of GlbN-A is an exception; a histidine modeled in place of the wild-type leucine fulfills both requirements with few clashes. However, only the *trans* χ_1 rotameric state can form product. This restrictive geometry forces the polar imidazole ring to be in contact with the 4-vinyl group and protein hydrophobic groups, unfavorable interactions that weaken the affinity of the apoprotein for ferric heme. High-pH conditions do not improve binding, which leads us to conclude that histidine desolvation and steric hindrance are the primary causes of variant holoprotein instability. Low-pH conditions also reduce heme affinity, likely because histidine protonation is energetically disfavored in the nonpolar environment of the holoprotein. The quality of the NMR spectra did not allow for the determination of the ionization constant of His79 in the unreacted state.

The contrasting distribution of histidines near vinyls and propionates illustrates clearly the influence of electrostatics (Figure S13 of the Supporting Information) on heme packing. In natural *b* heme proteins, however, the effects of introducing a bulky polar or charged residue in or near a heme pocket can be moderated with compensatory mutations and the luxury of an evolutionary time scale. In this light, the depletion of histidines near heme vinyl groups may be caused by physicochemical properties other than charge and polarity. Because the imidazole ring is an excellent ligand for ferric and ferrous heme iron, removing histidines from heme binding sites minimizes the risk of misligation during folding. The facile histidine−heme PTM in the L79H GlbN variants suggests that reactions leading to aberrant covalent attachment of chromophores are another potential source of pressure eliminating histidines near vinyls. In these two properties, ligation and reactivity, histidines resemble cysteines, which are thought to be preferentially avoided in *c*-type cytochrome sequences to ensure the formation of desired and homogeneous holoproteins.[12,45]

GlbN-A, GlbN-B, and GlbN-AB are chemically analogous and form under similar reducing conditions. We therefore hypothesize that the electrophilic addition mechanism proposed for GlbN-A is conserved in GlbN-B and GlbN-AB. Accordingly, the nucleophilic histidine (His117 or His79) attacks a vinyl with its Nε2 atom, the common *R* stereochemistry apparently stemming from a protonated vinyl intermediate oriented in *trans* as in the ferric starting material. In support of the reactive residue delivering the proton, ferrous H117C GlbN is able to form the thioether linkage of a *c*-type cytochrome, linking the Cys117 Sγ atom to the heme 2-Cα atom,[20] but H117S GlbN is not modified in the reduced state (data not shown), consistent with the high energetic cost of deprotonating the serine hydroxyl group. Additionally, because water does not compete efficiently with the side chain nucleophile and does not add to the vinyl group in any of

dx.doi.org/10.1021/bi400289e | *Biochemistry* 2013, 52, 3478−3488

the studied proteins, other geometrical requirements are inferred, for example, the proximity of the two reactive partners once heme protonation has occurred. A concerted protonation and attack mechanism can also account for the observations described above.

Optical data indicate that under similar conditions, cross-linking in both L79H/H117A and L79H GlbN occurs on a time scale several orders of magnitude slower than in the wild-type protein[20] (Figure 4A and Figure S8 of the Supporting Information). Rather than intrinsic difficulty in protonating the vinyl group, heme scavenging experiments (Figure 4B) and ^{1}H NMR spectra point to reduced affinity for the ferric and ferrous heme, i.e., shorter residence time in a reaction competent state, as being responsible for the observed deceleration. In L79H GlbN, the apparent monophasic conversion to product (Figure S8 of the Supporting Information) is consistent with the first cross-linking event being rate-determining and the second occurring faster than the first. Whether His117 or His79 initially attacks the heme cannot be distinguished with the current data. Importantly, the production of a double cross-link indicates that addition of an imidazole to one vinyl group does not inhibit reaction at the second vinyl group. It is especially clear from L79H GlbN that high heme affinity is not required for a stereospecific posttranslational modification.

Histidine–Heme Linkages versus Cysteine–Heme Linkages. Unlike the cysteine thiol reactant and thioether product of *c*-type cytochromes, the imidazole ring is titratable at physiological pH in its unmodified and modified forms. In GlbN, the kinetics of the PTM are dictated by the competing rates of vinyl protonation and acid-induced ferrous heme dissociation: between pH 9.5 and 6.0, the reaction is accelerated several orders of magnitude,[19] but an overly acidic pH causes heme loss. The properties of the histidine cross-linked product, which are under functional constraint, may depend on pH through a coupling of iron redox state and the modified histidine pK_a. Depending on local solvent accessibility, the alkylated histidine may remain ionizable at physiological pH, favoring charge heterogeneity at the heme active site. Thus, a histidine-modified heme may be undesirable in electron transfer proteins such as the *c*-type cytochromes.

In natural proteins, the preference for cysteine–heme attachment is likely to stem not only from the properties of the product but also from the versatility of the thiol group. Cysteine can react with the heme via reductive and oxidative mechanisms[13] and has additional options of deprotonation, methylation, phosphorylation, disulfide bridging (redox sensing), nitrosylation, and numerous other oxidative modifications.[46] This high reactivity allows multiple modes of regulation, some of which are critical in cytochrome *c* maturation.[13] In contrast, the opportunities for regulation of histidine–vinyl chemistry are more limited, principally to the iron redox state, pH, and histidine PTMs such as phosphorylation and methylation.

Because a cysteine at position 117 can serve as the nucleophile in GlbN,[20] and cysteine/histidine interchangeability has been documented in the heme chaperone CcmE,[47,48] the advantages of a histidine–heme bond over a cysteine–heme bond should also be considered. Under high oxidative and nitrosative stress, conditions that many cyanobacteria encounter, undesirable cysteine modifications may interfere with specific covalent heme attachment.[49] We proposed that the histidine–heme linkage is a solution to this problem in *Synechococcus* sp. PCC 7002.[8] Furthermore, cysteine tends to react with non-heme molecules containing vinyl groups, as demonstrated by spontaneous attachment of biliverdin IXα to phytochromes in vitro,[50,51] or ethylidine groups found in common cyanobacterial chromophores such as phycocyanobilin.[52] A histidine may be preferred over a cysteine in GlbN to limit these types of side reactions.

In conclusion, this study highlights the fact that heme vinyl groups are capable of spontaneous reaction with histidines to yield products similar to *c*-type cytochromes. This chemistry can occur even in highly destabilized proteins. In addition to providing opportunities for a comparative study of cysteine- and histidine-modified hemes and the consequences of such PTMs, histidine–heme attachment holds promise for the rational production of stable, artificial proteins containing a covalently bound heme. Interesting prospects include the design of redox protein switches responding to the reacted histidine's ionization state.

■ ASSOCIATED CONTENT

Supporting Information

Additional figures and tables. This material is available free of charge via the Internet at http://pubs.acs.org.

■ AUTHOR INFORMATION

Corresponding Author

*T. C. Jenkins Department of Biophysics, Johns Hopkins University, Baltimore, MD 21218. Telephone: (410) 516-7019. Fax: (410) 516-4118. E-mail: lecomte_jtj@jhu.edu.

Funding

This work was supported by National Science Foundation Grant MCB 084339. L.G. was supported by National Science Foundation Grant DBI 1005027.

Notes

The authors declare no competing financial interest.

■ ACKNOWLEDGMENTS

We thank Christopher Falzone for careful reading of the manuscript and Ananya Majumdar for assistance with the NMR experiments.

■ ABBREVIATIONS

DT, sodium dithionite; GlbN, *Synechocystis* sp. PCC 6803 hemoglobin without heme posttranslational modification; GlbN-A, GlbN with a bond between His117 Nε2 and heme 2-Cα; GlbN-B, GlbN with a bond between His79 Nε2 and heme 4-Cα; GlbN-AB, GlbN with a bond between His117 Nε2 and heme 2-Cα and a bond between His79 Nε2 and heme 4-Cα; lr, long-range; Mb, myoglobin.

■ REFERENCES

(1) Lippard, S. J., and Berg, J. M. (1994) *Principles of Bioinorganic Chemistry*, University Science Books, Mill Valley, CA.

(2) Salemme, F. R. (1977) Structure and function of cytochromes *c*. *Annu. Rev. Biochem. 46*, 299–329.

(3) Pettigrew, G. W., and Moore, G. R., Eds. (1991) *Cytochromes c: Evolutionary, Structural, and Physicochemical Aspects*, Springer-Verlag, Berlin.

(4) Colas, C., and Ortiz de Montellano, P. R. (2003) Autocatalytic radical reactions in physiological prosthetic heme modification. *Chem. Rev. 103*, 2305–2332.

(5) Battistuzzi, G., Stampler, J., Bellei, M., Vlasits, J., Soudi, M., Furtmuller, P. G., and Obinger, C. (2011) Influence of the covalent

heme-protein bonds on the redox thermodynamics of human myeloperoxidase. *Biochemistry 50*, 7987−7994.
(6) Vinogradov, S. N., and Moens, L. (2008) Diversity of globin function: Enzymatic, transport, storage, and sensing. *J. Biol. Chem. 283*, 8773−8777.
(7) Vu, B. C., Jones, A. D., and Lecomte, J. T. J. (2002) Novel histidine-heme covalent linkage in a hemoglobin. *J. Am. Chem. Soc. 124*, 8544−8545.
(8) Scott, N. L., Xu, Y., Shen, G., Vuletich, D. A., Falzone, C. J., Li, Z., Ludwig, M., Pond, M. P., Preimesberger, M. R., Bryant, D. A., and Lecomte, J. T. J. (2010) Functional and structural characterization of the 2/2 hemoglobin from *Synechococcus* sp. PCC 7002. *Biochemistry 49*, 7000−7011.
(9) Smagghe, B. J., Trent, J. T., III, and Hargrove, M. S. (2008) NO dioxygenase activity in hemoglobins is ubiquitous in vitro, but limited by reduction in vivo. *PLoS One 3*, e2039.
(10) Barker, P. D., and Ferguson, S. J. (1999) Still a puzzle: Why is haem covalently attached in *c*-type cytochromes? *Structure 7*, R281−R290.
(11) Allen, J. W., Barker, P. D., Daltrop, O., Stevens, J. M., Tomlinson, E. J., Sinha, N., Sambongi, Y., and Ferguson, S. J. (2005) Why isn't 'standard' heme good enough for *c*-type and d_1-type cytochromes? *Dalton Trans.*, 3410−3418.
(12) Bowman, S. E., and Bren, K. L. (2008) The chemistry and biochemistry of heme *c*: Functional bases for covalent attachment. *Nat. Prod. Rep. 25*, 1118−1130.
(13) Kranz, R. G., Richard-Fogal, C., Taylor, J. S., and Frawley, E. R. (2009) Cytochrome *c* biogenesis: Mechanisms for covalent modifications and trafficking of heme and for heme-iron redox control. *Microbiol. Mol. Biol. Rev. 73*, 510−528.
(14) Stevens, J. M., Uchida, T., Daltrop, O., and Ferguson, S. J. (2005) Covalent cofactor attachment to proteins: Cytochrome *c* biogenesis. *Biochem. Soc. Trans. 33*, 792−795.
(15) Vu, B. C., Vuletich, D. A., Kuriakose, S. A., Falzone, C. J., and Lecomte, J. T. J. (2004) Characterization of the heme-histidine cross-link in cyanobacterial hemoglobins from *Synechocystis* sp. PCC 6803 and *Synechococcus* sp. PCC 7002. *J. Biol. Inorg. Chem. 9*, 183−194.
(16) Hoy, J. A., Smagghe, B. J., Halder, P., and Hargrove, M. S. (2007) Covalent heme attachment in *Synechocystis* hemoglobin is required to prevent ferrous heme dissociation. *Protein Sci. 16*, 250−260.
(17) Pond, M. P., Majumdar, A., and Lecomte, J. T. J. (2012) Influence of heme post-translational modification and distal ligation on the backbone dynamics of a monomeric hemoglobin. *Biochemistry 51*, 5733−5747.
(18) Simonneaux, G., and Bondon, A. (2005) Mechanism of electron transfer in heme proteins and models: The NMR approach. *Chem. Rev. 105*, 2627−2646.
(19) Preimesberger, M. R., Pond, M. P., Majumdar, A., and Lecomte, J. T. J. (2012) Electron self-exchange and self-amplified posttranslational modification in the hemoglobins from *Synechocystis* sp. PCC 6803 and *Synechococcus* sp. PCC 7002. *J. Biol. Inorg. Chem. 17*, 599−609.
(20) Nothnagel, H. J., Preimesberger, M. R., Pond, M. P., Winer, B. Y., Adney, E. M., and Lecomte, J. T. J. (2011) Chemical reactivity of *Synechococcus* sp. PCC 7002 and *Synechocystis* sp. PCC 6803 hemoglobins: Covalent heme attachment and bishistidine coordination. *J. Biol. Inorg. Chem. 16*, 539−552.
(21) Nothnagel, H. J., Love, N., and Lecomte, J. T. J. (2009) The role of the heme distal ligand in the post-translational modification of *Synechocystis* hemoglobin. *J. Inorg. Biochem. 103*, 107−116.
(22) Lecomte, J. T. J., Scott, N. L., Vu, B. C., and Falzone, C. J. (2001) Binding of ferric heme by the recombinant globin from the cyanobacterium *Synechocystis* sp. PCC 6803. *Biochemistry 40*, 6541−6552.
(23) Scott, N. L., and Lecomte, J. T. J. (2000) Cloning, expression, purification, and preliminary characterization of a putative hemoglobin from the cyanobacterium *Synechocystis* sp. PCC 6803. *Protein Sci. 9*, 587−597.
(24) Teale, F. W. J. (1959) Cleavage of heme-protein link by acid methylethylketone. *Biochim. Biophys. Acta 35*, 543.
(25) de Duve, C. (1948) A spectrophotometric method for the simultaneous determination of myoglobin and hemoglobin in extracts of human muscle. *Acta Chem. Scand. 2*, 264−289.
(26) Antonini, E., Brunori, M., Caputo, A., Chiancone, E., Rossi-Fanelli, A., and Wyman, J. (1964) Studies on the structure of hemoglobin. III. Physicochemical properties of reconstituted hemoglobins. *Biochim. Biophys. Acta 79*, 284−292.
(27) Antonini, E., and Brunori, M. (1971) *Hemoglobin and myoglobin in their reactions with ligands*, Vol. *12*, North-Holland, Amsterdam.
(28) Cavanagh, J., Fairbrother, W. J., Palmer, A. G. I., and Skelton, N. J. (1996) *Protein NMR Spectroscopy. Principles and Practice*, Academic Press, San Diego.
(29) Kadkhodaei, M., Hwang, T. L., Tang, J., and Shaka, A. J. (1993) A simple windowless mixing sequence to suppress cross-relaxation in TOCSY experiments. *J. Magn. Reson., Ser. A 105*, 104−107.
(30) Inubushi, T., and Becker, E. D. (1983) Efficient detection of paramagnetically shifted NMR resonances by optimizing the WEFT pulse sequence. *J. Magn. Reson. 51*, 128−133.
(31) Pelton, J. G., Torchia, D. A., Meadow, N. D., and Roseman, S. (1993) Tautomeric states of the active-site histidines of phosphorylated and unphosphorylated IIIGlc, a signal-transducing protein from *Escherichia coli*, using two-dimensional heteronuclear NMR techniques. *Protein Sci. 2*, 543−558.
(32) Delaglio, F., Grzesiek, S., Vuister, G. W., Zhu, G., Pfeifer, J., and Bax, A. (1995) NMRPipe: A multidimensional spectral processing system based on UNIX pipes. *J. Biomol. NMR 6*, 277−293.
(33) Goddard, T. D., and Kneller, D. G. (2006) *SPARKY 3*, University of California, San Francisco.
(34) Wishart, D. S., Bigam, C. G., Yao, J., Abildgaard, F., Dyson, H. J., Oldfield, E., Markley, J. L., and Sykes, B. D. (1995) ^{1}H, ^{13}C and ^{15}N chemical shift referencing in biomolecular NMR. *J. Biomol. NMR 6*, 135−140.
(35) Bernstein, F. C., Koetzle, T. F., Williams, G. J., Meyer, E. F., Jr., Brice, M. D., Rodgers, J. R., Kennard, O., Shimanouchi, T., and Tasumi, M. (1977) The Protein Data Bank: A computer-based archival file for macromolecular structures. *J. Mol. Biol. 112*, 535−542.
(36) http:/www.rcsb.org/ (accessed December 2012).
(37) Hamelryck, T., and Manderick, B. (2003) PDB parser and structure class implemented in Python. *Bioinformatics 19*, 2308−2310.
(38) Hoy, J. A., Kundu, S., Trent, J. T., III, Ramaswamy, S., and Hargrove, M. S. (2004) The crystal structure of *Synechocystis* hemoglobin with a covalent heme linkage. *J. Biol. Chem. 279*, 16535−16542.
(39) Vu, B. C., Nothnagel, H. J., Vuletich, D. A., Falzone, C. J., and Lecomte, J. T. J. (2004) Cyanide binding to hexacoordinate cyanobacterial hemoglobins: Hydrogen bonding network and heme pocket rearrangement in ferric H117A *Synechocystis* Hb. *Biochemistry 43*, 12622−12633.
(40) Scott, N. L., Falzone, C. J., Vuletich, D. A., Zhao, J., Bryant, D. A., and Lecomte, J. T. J. (2002) The hemoglobin of the cyanobacterium *Synechococcus* sp. PCC 7002: Evidence for hexacoordination and covalent adduct formation in the ferric recombinant protein. *Biochemistry 41*, 6902−6910.
(41) Lee, D., Pervushin, K., Bischof, D., Braun, M., and Thöny-Meyer, L. (2005) Unusual heme-histidine bond in the active site of a chaperone. *J. Am. Chem. Soc. 127*, 3716−3717.
(42) Marzocchi, M. P., and Smulevich, G. (2003) Relationship between heme vinyl conformation and the protein matrix in peroxidases. *J. Raman Spectrosc. 34*, 725−736.
(43) http://www.bmrb.wisc.edu/ (accessed October 2012).
(44) Pearson, A. R., Elmore, B. O., Yang, C., Ferrara, J. D., Hooper, A. B., and Wilmot, C. M. (2007) The crystal structure of cytochrome P460 of *Nitrosomonas europaea* reveals a novel cytochrome fold and heme-protein cross-link. *Biochemistry 46*, 8340−8349.
(45) Sawyer, E. B., and Barker, P. D. (2012) Continued surprises in the cytochrome *c* biogenesis story. *Protein Cell 3*, 405−409.

(46) Lecomte, J. T. J., and Falzone, C. J. (2013) Protein structure: Unusual covalent bonds. In *eLS*, John Wiley & Sons, Ltd., Chichester, U.K.
(47) Aramini, J. M., Hamilton, K., Rossi, P., Ertekin, A., Lee, H. W., Lemak, A., Wang, H., Xiao, R., Acton, T. B., Everett, J. K., and Montelione, G. T. (2012) Solution NMR structure, backbone dynamics, and heme-binding properties of a novel cytochrome *c* maturation protein CcmE from *Desulfovibrio vulgaris*. *Biochemistry 51*, 3705−3707.
(48) Goddard, A. D., Stevens, J. M., Rao, F., Mavridou, D. A., Chan, W., Richardson, D. J., Allen, J. W., and Ferguson, S. J. (2010) c-Type cytochrome biogenesis can occur via a natural Ccm system lacking CcmH, CcmG, and the heme-binding histidine of CcmE. *J. Biol. Chem. 285*, 22882−22889.
(49) Barker, P. D., Ferrer, J. C., Mylrajan, M., Loehr, T. M., Feng, R., Konishi, Y., Funk, W. D., MacGillivray, R. T., and Mauk, A. G. (1993) Transmutation of a heme protein. *Proc. Natl. Acad. Sci. U.S.A. 90*, 6542−6546.
(50) Lamparter, T., Michael, N., Mittmann, F., and Esteban, B. (2002) Phytochrome from *Agrobacterium tumefaciens* has unusual spectral properties and reveals an N-terminal chromophore attachment site. *Proc. Natl. Acad. Sci. U.S.A. 99*, 11628−11633.
(51) Borucki, B., Seibeck, S., Heyn, M. P., and Lamparter, T. (2009) Characterization of the covalent and noncovalent adducts of Agp1 phytochrome assembled with biliverdin and phycocyanobilin by circular dichroism and flash photolysis. *Biochemistry 48*, 6305−6317.
(52) Scheer, H., and Zhao, K. H. (2008) Biliprotein maturation: The chromophore attachment. *Mol. Microbiol. 68*, 263−276.